Int J Adv Manuf Technol (2013) 68:1055–1061
DOI 10.1007/s00170-013-4896-y

ORIGINAL ARTICLE

Mathematical modeling and verification of pulse electrochemical micromachining of microtools

Abishek B. Kamaraj · M. M. Sundaram

Received: 8 November 2012 / Accepted: 6 March 2013 / Published online: 22 March 2013

Abstract Pulse electrochemical micromachining (PECMM) is an unconventional manufacturing method suitable for the production of micro-sized components on a wide range of electrically conductive materials. PECMM in this study has been used to manufacture microtools. The non-contact nature of PECMM has necessitated the modeling of the process to estimate the anodic profile (microtool profile). This paper presents a mathematical model for predicting the diameter of the microtools fabricated by PECMM process. Tungsten microtools of diameters less than 100 μm were fabricated using an in-house built microelectrochemical machining system. Experimental results confirm the theoretical prediction of reduction in tool diameter with respect to increasing machining time. Further, from the experimental verification, it was found that the deviations in the tool diameters were within 9 % of the theoretical predictions.

Keywords Electrochemical machining · Mathematical model · Micromachining · Microtool fabrication · Tungsten

1 Introduction

Product miniaturization has fueled the growth of micromanufacturing, especially in the fields of biomedical, automobile, health care, optics, and consumer electronics. This has triggered an ever-growing demand for micro-sized parts and novel methods to produce them on a wide variety of materials. Several non-lithography-based micromanufacturing processes, such as electro discharge machining (EDM), electrochemical machining (ECM), ultrasonic machining, and combinations of these machining processes that lead to hybrid machining, have been developed to address the demand for micromanufacturing on a wide variety of materials. These complementary micromachining processes need simple-shaped microtools as a prerequisite to fabricate the desired microfeatures. Microtool fabrication and handling pose several challenges due to their size. ECM is one of the micromachining processes that can be used to make microtools. The introduction of pulsed current to the process of ECM has enabled ECM to be used in microfabrication with nanoscale precision [1]. Accurate machining of microfeatures of required dimensions is a challenging task in ECM due to its non-contact nature of machining. To overcome this limitation, this paper presents a method to predict the final dimension of the machined feature by modeling the interelectrode gap in the ECM. Using the mathematical model developed in this work, the diameter of a microtool fabricated by pulse electrochemical micromachining (PECMM) was predicted, and the model was validated using an in-house built micro ECM setup.

A. B. Kamaraj · M. M. Sundaram (✉)
Micro and Nano Manufacturing Laboratory, School of Dynamic Systems, University of Cincinnati, Cincinnati, OH, USA
e-mail: murali.sundaram@uc.edu

2 Literature review

ECM is a non-traditional machining process in which material is removed by the mechanism of targeted anodic dissolution during an electrolysis process. The anodic dissolution rate, which is governed by Faraday's laws of electrolysis, depends upon the electrochemical properties of the metal, electrolyte properties, and the type of electric current/voltage supplied [2]. The cathode remains unaffected during the ECM process. This gives ECM an advantage over many other processes because there is no tool wear or any other issue, such as distortion due to residual stress, that may warrant tool change [3].

PECMM is a variation of ECM, suitable for the micro-scale fabrication, where a pulsed power is used instead of DC current. PECMM leads to higher machining accuracy, better process stability, and suitability for control. These advantages are due to the improved electrolyte flow condition in the interelectrode gap, enhanced localization of

anodic dissolution, and small and stable gaps found in PECMM. The PECMM process has been used in the fabrication of microholes [4], microslots [5], and microtools [6]. Pulsed current has also found applications in the electrochemical co-deposition (plating) of microtools [7].

Several studies have been conducted on the fabrication of microelectrodes using ECM. The influence of vibration on the microtool fabrication using ECM was studied in [8]. High aspect ratio microtools/electrodes are used for biomedical, micromanufacturing, and micrometrology applications. Tungsten microtools were fabricated using pulse electrochemical machining (PECM) in [9, 10] and the tools were used to drill microholes using ECM. Tool handling issues are minimized with the in-process manufacturing of tools used in ECM. Ultra high aspect ratio microtools (>450) were produced with pulsed ECM using reverse currents [11]. These tools can be used to machine high aspect ratio microholes using ECM or EDM. They can also be used as metrology probes for measuring ultra-deep features. These high aspect ratio electrodes also find biomedical applications as neural implants [12]. They are used as minimally invasive neural sensors for treating physical conditions such as the aftermath of a stroke, disease, or other neural problems. Another application of these high aspect ratio electrodes is as cochlear implant electrodes for patients with cochlear auditory disorders. The surface finish achieved through this process was 0.3 μm. The surface roughness of microtools was also improved with the use of ECM combined with a honing process to get very fine finish (Ra—0.02 μm) [13].

Achievement of the required shape of a workpiece within a given tolerance limit is a critical requirement in any machining process. The non-contact nature of ECM has resulted in the need for the modeling of the ECM process for the prediction of anodic profile during the microtool fabrication by PECMM. The changes in electrolyte conductivity and anodic electrochemical behavior determine the dynamic change in the interelectrode gap in ECM [14]. These changes in the interelectrode gap reflect the changes in the anode surface profile. An incorrect assessment of the gap variation during the process of machining will result in an improper workpiece profile and may also cause short circuiting, which is detrimental to the machining process [2].

Several mathematical and analytical models have been developed to analyze the ECM and PECM processes as discussed below. A variation of ECM is the ECM die-sinking in steady-state process. In this process, the tool profile is a 3-D negative image of the required surface profile. The tool is allowed to sink into the workpiece at a constant feed rate, until the required shape is obtained on the workpiece. Models developed for this process concentrate on the prediction of the equilibrium gap which is necessary to design the actual tool profile. The equilibrium gap size in a steady-state ECM process is given by

$$S_f = \kappa K_v \frac{U - E}{V_f} \quad (1)$$

where κ is the electrolyte conductivity, K_v is the electrochemical machinability coefficient defined as the volume of material dissolved per unit electrical charge, U is the working voltage, E is the total overpotential of the electrode processes, and V_f is the vertical feed rate of the electrode [15]. The equilibrium gap calculated using the above model is used in the design of the tool, so that the required workpiece profile is obtained.

Another process variation is ECM shaping. In this process, a universal simple-shaped tool (e.g., cylindrical rod) is moved along a specified path to obtain the required shape of the workpiece. One of the most important advantages of this process (unshaped tool), besides elimination of expensive electrodes of complicated shapes, is the increase in machining accuracy and in workpiece surface quality. This improvement is achieved by the decrease of the working area of the electrode that significantly reduces the influence of heat and gas generation on the electrolyte properties in the interelectrode gap. This makes the conditions of dissolution more uniform and allows machining with smaller interelectrode gap [16]. The ECM shaping system was modeled in [17], where a universal tool electrode of a simple shape is moved along a complex path to obtain the required shape of the workpiece. This model was simulated in a computer and the workpiece shape evolution was determined using the finite difference method.

Modeling of pulse ECM for macro-scale machining has been reported in [18] and the gap dynamics were analyzed for non-steady-state conditions. The effect of these process parameters like pulse timing, initial gap, and electrolyte conditions were analyzed. In this model, the gap variation was modeled after one pulse duration and was shown that PECM has smaller interelectrode gap requirements, resulting in more accurate machining and better tool design. Modeling ECM

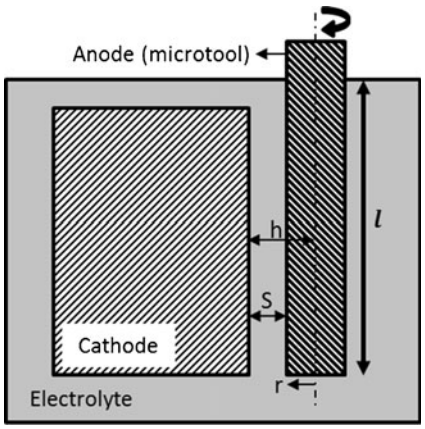

Fig. 1 Tool fabrication schematic

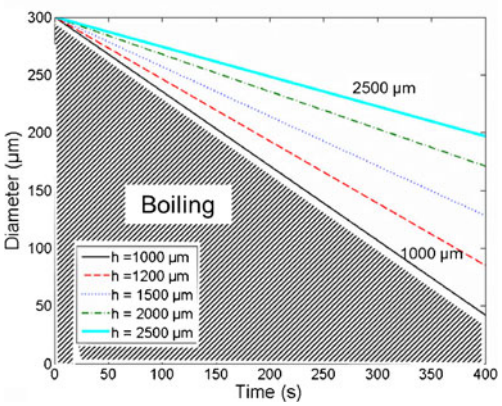

Fig. 2 Theoretical prediction of tool diameter with machining gap and time

using a rotating electrode has been reported in [19]. In this work, the tool electrode was rotated and the gap dynamics were analyzed to give the optimum tool feed rate and other machining parameters. The advantages in using rotating electrode according to this study were the improved flow characteristics due to rotation resulting in lower pressure of the inlet electrolyte.

In another work, the rate of change of the interelectrode gap was modeled for an electrochemical deburring process. This model was used to determine the variation of the burr height, the deburring time, and the loss of base material for various parametric combinations in electrochemical deburring process [20]. This model is limited to direct current and does not take into account the pulse current used in micro ECM. For the electrochemical finishing process, the variation of the gap with pulse current was modeled in [21]. The model was for a rotating anode (workpiece) and stationary cathode. Apart from predicting the gap, the model goes on to suggest that the surface roughness values after the finishing process are completed [21]. A review of the mass transfer issues in ECM with the problems associated with the micro- and nanoscale ECM is given in [22]. Numerical modeling of the ECM process considering the hydrodynamics involved in the process was studied in [23]. The end anode shape resulting after ECM using a triangular-shaped cathode was modeled in this study. A similar model for curved cathode considering electrolyte condition over curved surfaces was modeled in [24]. Cathode design in die-sinking ECM with shaped electrodes is important because the inverse shape of the cathode is what is obtained on the workpiece (anode). A convergence analysis on the performance of finite element method as a tool for cathode design modeling is given in [25]. Modeling of microwire electrodes produced using ECM is reported in [26]. These electrodes were then used in microwire electrochemical machining. Simulation of the heat generated during the ECM process and its effective dissipation using electrolytic flow was studied in [27]. It was found that a hollow cathode and pulse voltages help in the effective control of the heat generated. Numerical simulation of the ECM process taking into account the temperature effects was studied in [28, 29], and the temperature distribution was found to have an influence on the shape of the anode with regions of higher temperature showing higher machining rates.

All the models discussed so far deal with the modeling of gap dynamics during ECM and PECM, but none of these are specific to the fabrication of microtools using PECMM. In this paper, the change in interelectrode gap has been modeled between a flat plate cathode and a rotating anode. The variation of the microtool diameter, with respect to various machining parameters such as initial gap and machining, and time has been analyzed using the mathematical model.

3 Process modeling

The schematic of the PECM process for the fabrication of microtools is illustrated in Fig. 1, where r is the radius of the rotating anode, l is the length of the anode immersed in the electrolyte, h represents the average gap distance of a given point on the peripheral surface of the rotating anode (microtool) to form the vertical surface of the cathode, and S is the closest distance between the outermost generatrix of anode and the nearest vertical surface of the cathode as shown in Fig. 1. It should be noted that the value of h remains constant even with change in S and r during the process of machining.

Assumptions considered while arriving at a model for the PECM process are

- Current efficiency (η), overpotential (ΔU), and electrolytic conductivity (κ_e) are considered to be constants during the process of machining.

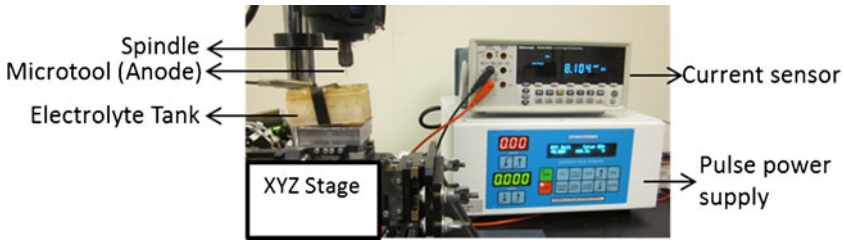

Fig. 3 Experimental setup

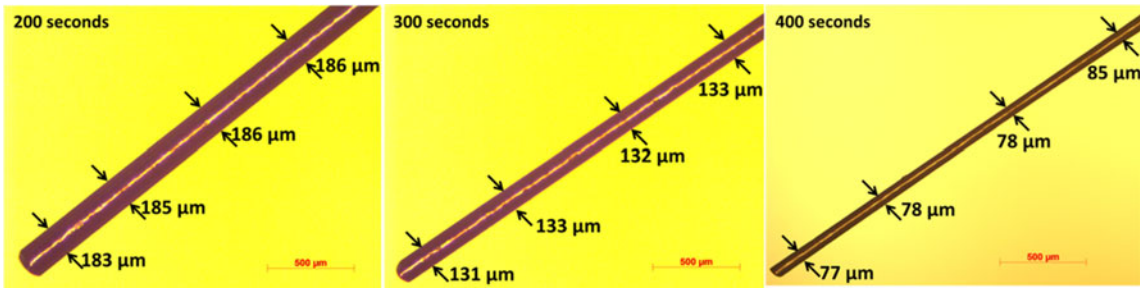

Fig. 4 Microtool after machining for 200, 300, and 400 s

- Joule heating effects are neglected as the machining is considered to be in the microscale and the microtool is in constant rotation. The electrolyte temperature increase observed was only 5 K, validating the assumption.
- The effect of the bubble layer on the electrolyte conductivity (κ_e) is determined by the Bruggeman equation: $\kappa_e=\kappa_0(1+\alpha(\Delta T))(1-\beta)^{1.5}$, where κ_0 is the conductivity of the bulk electrolyte, α is the temperature coefficient of the electrolyte conductivity, β is the temperature difference in Kelvin, and β is the void fraction of the gas phase due to bubble formation.
- Current density is assumed to be uniform along the full length of the microtool.

Electrolyte flow and pressure effects have been neglected, since the movement of electrolyte is only due to the rotation of the anode.

The volumetric material removal rate (ν) for electrochemical processes is governed by Faraday's law and can be calculated as follows [2, 30]

$$\nu = \eta K_v I \tag{2}$$

where I is the current, η is the current efficiency, and K_v is the volumetric electrochemical equivalent, which is the volume of anodic material removed per unit electrical charge. In the case of microtools, the volume can be expressed as $v=\pi r^2 l$.

$$\nu = 2\pi l r \frac{dr}{dt} \tag{3}$$

For constant electrolyte conductivity, Ohm's law gives the relationship between the current and the voltage as

$$J = \frac{\kappa_e V}{h} \tag{4}$$

where J is the mean current density, κ_e is the electrolyte conductivity, V is the voltage applied across the electrodes, and $h=S+r$ is the mean gap between the electrodes. It should be noted that h is used instead of S in this equation for the average current density.

Conductivity (κ_e) can be expressed in terms of the bulk electrolyte conductivity (κ_0) and the void fraction (β) as $\kappa_e = \kappa_0(1+\alpha(\Delta T))(1-\beta)^{1.5}$ by use of the Bruggeman equation. Due to the micron scale involved, the void fraction is assumed uniform over the gap with a value of 0.5 [31]. The current I is related to the current density as

$$I = JA = \frac{\kappa_e V}{h}(2\pi l r) \tag{5}$$

where A is the surface area of the immersed microtool (assuming constant current density).

From Eqs. 2, 3, and 5, a relationship between the rate of change in tool radius and the machining parameters can be established as

$$\frac{dr}{dt} = \eta K_v \frac{\kappa_e V}{h} \tag{6}$$

Table 1 PECMM parameters

Voltage	Forward—10 V
	Reverse—10 V
Anode	Tungsten rod of Ø300µm
Cathode	0.5-mm-thick stainless steel plate
Electrolyte	10 % wt. sodium chloride solution
Average current	0.02–0.07 A
Pulse period	15 ms
Duty cycle	Forward 33 %
	Reverse 33 %
Spindle rotation	200 rpm
Interelectrode gap (S)	1,000 µm
Immersed tool length (l)	4 mm

Table 2 Efficiency calculation

Time (s)	200	300	400
Average current measured (A)	0.062	0.056	0.039
m (g/s)	1.93E−05	1.82E−05	1.23E−05
Current efficiency	0.98	1.02	0.99

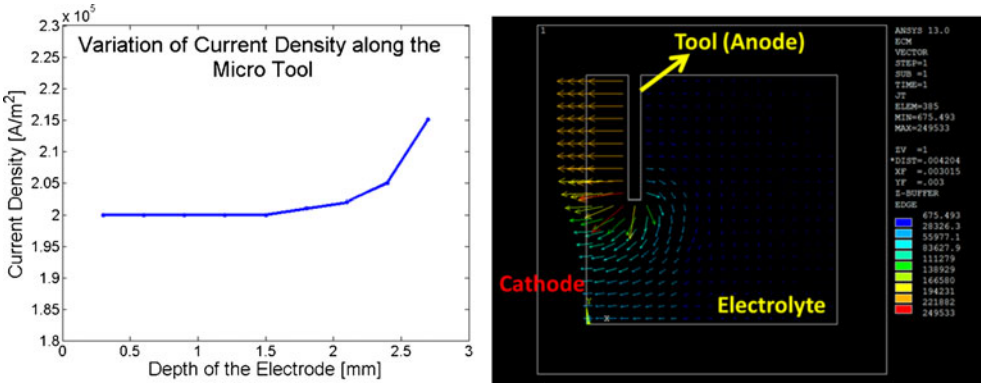

Fig. 5 (*Left*) Current density along the side of the microtool, showing increasing current density along the depth of the tool immersed in the electrolyte; (*right*) current density vector plot

Change in tool radius over a time period t can be obtained by integrating Eq. 6 over a time period of t, with initial radius r_0 and final radius r_t

$$r_0 - r_t = \int_0^t \eta K_v \frac{\kappa_e V}{h} dt \tag{7}$$

The effective machining time is determined by the pulse on time t_p and the pulse frequency f. It should be noted that no machining happens during the pulse off time. Thus,

$$r_0 - r_t = \sum_0^n \int_0^{t_p} \eta K_v \frac{\kappa_e V}{h} dt \tag{8}$$

where n is the number of pulses in the time period t, which is the product of pulse frequency and time t ($n=t\times f$). Assuming that the voltage (V), efficiency (η), and electrolyte conductivity (κ_e) remain constant during the pulse duration [32], we get

$$r_0 - r_t = \eta K_v \frac{\kappa_e V}{h} t_p f t \tag{9}$$

The final diameter (D_t) of the microtool can be derived from Eq. 9 as

$$D_t = D_0 - 2\eta K_v \frac{\kappa_e V}{h} t_p f t \tag{10}$$

The model prediction of the reduction of diameter, with respect to machining time and gap, is plotted in Fig. 2. The machining parameters used in the analysis are D_0=300 μm, η=100 %, K_v=1.7×10^{-11} m^3/As (for tungsten), β=0.5, κ_0= 14 A/Vm (10 % NaCl at 300 K), V=10 V, t_p=5 ms, α=0. 03 K^{-1}, Δ=5 K, and f=66.66 Hz.

Theoretical predictions shown above suggest the usage of smaller values of average interelectrode gap (h) for faster reduction in tool diameter with increasing machining time. However, boiling of electrolyte was observed for average interelectrode gap values lower than 500 μm. This observation is in line with literature on boiling effects becoming significant at lower levels of interelectrode gaps [33]. Thus, a minimum average interelectrode gap of 1,000 μm was maintained in this study to avoid the boiling effects.

4 Experimental verification

The setup used for the experimental verification of the PECMM process model is shown in Fig. 3. The cathode is immersed in electrolyte in a tank mounted on an XYZ stage. The stage provides precise motion control in the longitudinal, lateral, and axial directions. The spindle holding the anode rotates at a constant rate of 200 rpm during all the experiments. The pulse power supply provides the required pulsed voltage and current for machining. A multimeter is connected in series with the power supply and is used as a current sensor to monitor and record the current variation during the machining process. After the anode is positioned with respect to the cathode at the required interelectrode gap, the power supply is turned on to provide a pulse voltage. The experimental parameters used in this study are given in Table 1. Bipolar current (reverse pulses) was

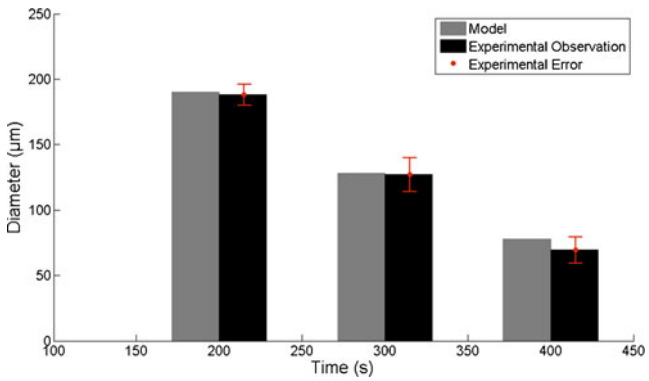

Fig 6 Comparison of experimental results and model prediction

used during the microtool fabrication process, which eliminated the issue of tungsten passivation [11, 34].

4.1 Current variation and efficiency

When the current supplied during ECM is not effectively used in the process of machining, the efficiency of the ECM process decreases. Some of the causes for lower current efficiency are passivation, high current density, anodic bubble generation, and electrolyte flow [2, 35]. Higher current efficiency may be observed if the metal dissolves at a different valence state than the one expected, or if the conductivity of the electrolyte increases due to the addition of ions and temperature rise. Since analytical models of current efficiency are not available, experimental values have to be collected and used in the model verification. The current efficiency can be calculated as

$$\text{Current efficiency} = \frac{m}{\left(\frac{A}{zF}\right)I} \tag{11}$$

where m is the observed material removal rate. The denominator denotes the theoretical material removal rate expected based on Faradays law. A is the atomic weight, z is the valency by which the metal dissolves, F is Faraday's constant, and I is the average current supplied (obtained from current sensor readings). The efficiency value was calculated based on experimental observations of the machining process, which was replicated three times. The valency of tungsten dissolution is 6 at anodic potentials [36]. The time of machining was 200, 300, and 400 s. All of the other parameters were the same as given in Table 1. Table 2 gives the observations for the current efficiency calculation used in tungsten microtool fabrication.

The average current values decrease over a period of time due to the reduction in tool diameter. This is in accordance with the modified Ohm's law given in Eq. 5. The efficiency value was almost constant (variation within 2 %), as shown in Table 2.

4.2 Model verification—variation with time

In order to validate the theoretical model, experiments were conducted to find the variation in the microtool diameter with respect to the machining time. The initial gap (S) was maintained at 1 mm for all of the experiments. Each run was replicated three times, and the average value of the diameter noted. The tool diameter was measured at four different positions over the length of the microelectrode, as shown in Fig. 4 for each of the microtool produced. The average of these four values was recorded as the mean microtool diameter.

The small variations in the tool diameter along the length of the tool are not predicted by the model developed in this work because one of the simplification assumptions made in this model development is that the "Current density is assumed to be uniform along the full length of the microtool." However, a finite element simulation of the current density along the sides of the microtool reveals that the current density gradually increases along the depth of the immersed tool as shown in Fig. 5. This variation in the current density causes gradual increase in the material removal and slight variation in the diameter of the tool produced.

Figure 6 shows the comparison of the theoretical predictions and experimental values of tool diameter with increasing machining time. The model predictions were within 9 % deviation from the actual observed microtool diameters.

5 Conclusion

A mathematical model was developed in this work to predict the diameter of the microtools fabricated using the PECMM process. Tungsten microtools of diameters less than 200 μm were fabricated using an in-house built microelectrochemical machining system. Theoretical predictions suggest the usage of smaller values of average interelectrode gap for faster reduction in tool diameter with increasing machining time. However, for the experimental conditions used in this study, too small values (500 μm and less) of average interelectrode gap resulted in boiling of electrolyte. Experimental verification of the mathematical model revealed that the experimental results are in confirmation with theoretical prediction of reduction in tool diameter with respect to increasing machining time. The deviations in the tool diameters were found to be within 9 % of the theoretical predictions.

Acknowledgments Financial support provided by the National Science Foundation under grant no CMMI–1120382 and by the University of Cincinnati under the URC Faculty Research Grant program is acknowledged.

References

1. Schuster R, Kirchner V, Allongue P, Ertl G (2000) Electrochemical micromachining. Science 289(5476):98–101. doi:10.1126/science.289.5476.98
2. McGeough JA (1974) Principles of electrochemical machining. Chapman and Hall, London
3. Bo Hyun K, Shi Hyoung R, Deok Ki C, Chong Nam C (2005) Micro electrochemical milling. J Micromech Microeng 15(1):124
4. Mithu M, Fantoni G, Ciampi J (2011) The effect of high frequency and duty cycle in electrochemical microdrilling. Int J Adv Manuf Technol 55(9):921–933. doi:10.1007/s00170-010-3123-3
5. Kim BH, Na CW, Lee YS, Choi DK, Chu CN (2005) Micro electrochemical machining of 3D micro structure using dilute sulfuric acid. CIRP Ann Manuf Technol 54(1):191–194. doi:10.1016/s0007-8506(07)60081-x

6. Mathew R, James S, Sundaram MM (2010) Experimental study of micro tools fabricated by electrochemical machining. ASME Conf Proc 2010(49460):73–80
7. Dabholkar A, Sundaram MM (2012) Study of micro-abrasive tool-making by pulse plating using Taguchi method. Mater Manuf Process 27(11):1233–1238. doi:10.1080/10426914.2012.663143
8. Ghoshal B, Bhattacharyya B (2013) Influence of vibration on micro-tool fabrication by electrochemical machining. Int J Mach Tool Manuf 64:49–59. doi:10.1016/j.ijmachtools.2012.07.014
9. Liu Y, Zhu D, Zeng Y, Yu H (2010) Development of microelectrodes for electrochemical micromachining. Int J Adv Manuf Technol 55(1–4):195–203. doi:10.1007/s00170-010-3035-2
10. Fan Z-W, Hourng L-W, Wang C-Y (2010) Fabrication of tungsten microelectrodes using pulsed electrochemical machining. Precis Eng 34(3):489–496. doi:10.1016/j.precisioneng.2010.01.001
11. Mathew R, Sundaram MM (2012) Modeling and fabrication of micro tools by pulsed electrochemical machining. J Mater Process Technol 212(7):1567–1572. doi:10.1016/j.jmatprotec.2012.03.004
12. Kamaraj AB, Sundaram MM, Mathew R (2013) Ultra high aspect ratio penetrating metal microelectrodes for biomedical applications. Microsyst Technol 19(2):179–186. doi:10.1007/s00542-012-1653-3
13. Guo S, Guo ZN, Luo HP, Gu WC (2011) Experimental research of electrochemical mechanical polishing (ECMP) for micro tool electrode. Adv Mater Res 314–316:1846–1850. doi:10.4028/www.scientific.net/AMR.314-316.1846
14. Rajurkar KP, Wei B, Kozak J, McGeough JA (1995) Modelling and monitoring interelectrode gap in pulse electrochemical machining. CIRP Ann Manuf Technol 44(1):177–180. doi:10.1016/s0007-8506(07)62301-4
15. Kozak J, Rajurkar K, Makkar Y (2004) Selected problems of micro-electrochemical machining. J Mater Process Technol 149(1–3):426–431. doi:10.1016/j.jmatprotec.2004.02.031
16. Rajurkar KP, Levy G, Malshe A, Sundaram MM, McGeough J, Hu X, Resnick R, DeSilva A (2006) Micro and nano machining by electro-physical and chemical processes. CIRP Ann Manuf Technol 55(2):643–666. doi:10.1016/j.cirp.2006.10.002
17. Kozak J (1998) Mathematical models for computer simulation of electrochemical machining processes. J Mater Process Technol 76(Compendex):170–175
18. Kozak J, Rajurkar KP, Wei B (1994) Modelling and analysis of pulse electrochemical machining (PECM). J Eng Ind 116(3):316–323
19. Kozak J, Dabrowski L, Osman H, Rajurkar KP (1991) Computer modelling of electrochemical machining with rotating electrode. J Mater Process Technol 28(1–2):159–167. doi:10.1016/0924-0136(91)90215-z
20. Sarkar S, Mitra S, Bhattacharyya B (2004) Mathematical modeling for controlled electrochemical deburring (ECD). J Mater Process Technol 147(2):241–246
21. Ma N, Xu W, Wang X, Tao B (2010) Pulse electrochemical finishing: modeling and experiment. J Mater Process Technol 210(6–7):852–857. doi:10.1016/j.jmatprotec.2010.01.016
22. Volgin V, Davydov A (2012) Mass-transfer problems in the electrochemical systems. Russ J Electrochem 48(6):565–569. doi:10.1134/s1023193512060146
23. Minazetdinov NM (2009) A hydrodynamic interpretation of a problem in the theory of the dimensional electrochemical machining of metals. J Appl Math Mech 73(1):41–47. doi:10.1016/j.jappmathmech.2009.03.009
24. Minazetdinov NM (2009) A scheme for the electrochemical machining of metals by a cathode tool with a curvilinear part of the boundary. J Appl Math Mech 73(5):592–598. doi:10.1016/j.jappmathmech.2009.11.012
25. Zhiyong L, Zongwei N (2007) Convergence analysis of the numerical solution for cathode design of aero-engine blades in electrochemical machining. Chin J Aeronaut 20(6):570–576. doi:10.1016/s1000-9361(07)60084-3
26. Zhu D, Wang K, Qu NS (2007) Micro wire electrochemical cutting by using in situ fabricated wire electrode. CIRP Ann Manuf Technol 56(1):241–244. doi:10.1016/j.cirp.2007.05.057
27. Wu J, Wang H, Chen X, Cheng P, Ding G, Zhao X, Huang Y (2012) Study of a novel cathode tool structure for improving heat removal in electrochemical micro-machining. Electrochim Acta 75:94–100. doi:10.1016/j.electacta.2012.04.078
28. Deconinck D, Van Damme S, Deconinck J (2012) A temperature dependent multi-ion model for time accurate numerical simulation of the electrochemical machining process. Part I: theoretical basis. Electrochim Acta 60:321–328. doi:10.1016/j.electacta.2011.11.070
29. Deconinck D, Damme SV, Deconinck J (2012) A temperature dependent multi-ion model for time accurate numerical simulation of the electrochemical machining process. Part II: numerical simulation. Electrochim Acta 69:120–127. doi:10.1016/j.electacta.2012.02.079
30. Rajurkar KP, Kozak J, Wei B, McGeough JA (1993) Study of pulse electrochemical machining characteristics. CIRP Ann Manuf Technol 42(1):231–234. doi:10.1016/s0007-8506(07)62432-9
31. Loutrel SP, Cook NH (1973) A theoretical model for high rate electrochemical machining. J Eng Ind 95(4):1003–1008
32. Wei B (1994) Modeling and analysis of pulse electrochemical machining. University of Nebraska–Lincoln, Lincoln
33. Kozak J (2004) Thermal models of pulse electrochemical machining. Bull Pol Acad Sci Chem 52(4):313–320
34. Balsamy Kamaraj A, Dyer R, Sundaram MM (2012) Pulse electrochemical micromachining of tungsten carbide. In: ASME 2012 International Manufacturing Science and Engineering Conference (MSEC2012), University of Notre Dame, Notre Dame, IN, USA
35. Zhang Y (2010) Investigation into current efficiency for pulse electrochemical machining of nickel alloy. Thesis, University of Nebraska–Lincoln, Lincoln
36. Pourbaix M (1974) Atlas of electrochemical equilibria in aqueous solutions. NACE, Houston, p 644